

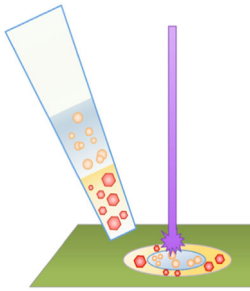
RESEARCH ARTICLE

DAPNe with micro-capillary separatory chemistry-coupled to MALDI-MS for the analysis of polar and non-polar lipid metabolism in one cell

Jason S. Hamilton,¹ Roberto Aguilar,¹ Robby A. Petros,² Guido F. Verbeck¹

¹Department of Chemistry, University of North Texas, Denton, TX, USA

²Department of Chemistry, Texas Women's University, Denton, TX, USA



cell is non-reproducible; therefore, a broad chemical analysis of metabolites is necessary and will be illustrated with the one-cell analysis of a single Snu-5 gastric cancer cell taken from a cellular suspension. The method presented here shows a broad partitioning dynamic range as a single-step method for lipid analysis demonstrating a decrease in ion suppression often present in MALDI analysis of lipids.

Keywords: MALDI, DAPNe, Nanomanipulation, One-cell

Received: 2 June 2016/Revised: 27 January 2017/Accepted: 31 January 2017/Published Online: 1 March 2017

Introduction

The cellular metabolome is a dynamic collection of metabolites considered to be small molecules of less than 1000 Da in molecular mass [1], including sugars, peptides, lipids, and other small molecules of varying hydrophilicity and lipophilicity [2, 3]. The cellular metabolome is considered to be a direct representation of a cell's phenotype and considered to be a measure of the immediate cellular responses brought about by changes in environment, disease state, or diet [4]. The responsive nature of the metabolome provides the opportunity for biomarker discovery through metabolomics and lipidomics [4–8]. However, the metabolome is an expansive set of molecules that can greatly vary in their physiochemical states, making single-platform analysis for polar and non-polar metabolite profiling difficult. The method presented here offers a demonstration of a solution through the simultaneous extraction and partitioning of polar and nonpolar lipids in an immiscible solvent system coupled to mass spectrometry

imaging (MSI) by matrix assisted laser desorption/ionization (MALDI) for single platform analysis.

Historically, the extraction of lipophilic and hydrophilic metabolites consists of multi-step extraction procedures using immiscible solvent systems of an organic and aqueous solvent to create a biphasic mixture. Lipids and nonpolar metabolites partition into the organic phase whereas polar metabolites partition into the aqueous phase. The phases are then collected separately to undergo further purification or re-extraction to ensure complete metabolite extraction [3]. The Folch and Bligh-Dyer methods are two of the most commonly used biphasic extraction methods and were developed to extract lipids into the organic phase while the aqueous phase was used for sample purification to remove non-lipids [9, 10]. The Folch et al. method uses a 2:1 chloroform/methanol ($\text{CHCl}_3/\text{MeOH}$) solvent system for the extraction of lipids followed by a 0.2 volume addition of water (H_2O) during a washing step to remove non-lipids [9]. The Bligh-Dyer et al. method uses an initial extraction solvent of 1:2 $\text{CHCl}_3/\text{MeOH}$ followed by the addition of 1:1 $\text{CHCl}_3/\text{H}_2\text{O}$ to induce a biphasic mixture and remove polar and nonlipid contaminants from the organic phase [10]. However, because polar metabolites are extracted into the

aqueous phase of the Folch and Bligh-Dyer methods, they are useful for metabolomics studies. Biphasic extraction methods using varying ratios of CHCl₃/MeOH/H₂O for the extraction of polar and nonpolar metabolites have been performed on mouse melanoma cells [11], blood parasites [12], bacterial and macrophage cells [13], urine, and plasma [14]. Several other groups used a modified extraction method by replacing CHCl₃ with methyl *tert*-butyl ether (MTBE) for the extraction of metabolites from plasma [15–17], mouse tissue [18], rat tissue [19], and serum spots, urine, and cerebrospinal fluid [20]. Methods have been developed to extract polar and nonpolar metabolites using monophasic systems to cut down on time and prepare for single platform analysis [21–23], but these systems often neglect the extraction of neutral lipids, as outlined in a comparison study of 12 such methods by Dietmar et al. [21].

Metabolomics experiments are most commonly performed using nuclear magnetic resonance (NMR) or mass spectrometry (MS) through direct injection of a crude sample or following separation by gas chromatography (GC-MS), capillary electrophoresis (CE-MS), or liquid chromatography (LC-MS) [3, 4, 8, 24]. NMR has several advantages for its use in metabolomics; it is non-destructive, biological samples can be analyzed in their natural state, results are highly reproducible, and metabolites can be quantified down to the micromolar scale [3, 4, 8]. However, NMR is limited by its sensitivity, as metabolites of sub-micromolar concentrations are not detected [4, 8]. Mass spectrometry (MS) provides picomolar sensitivity, metabolites can be quantified, structural information is provided, and isomeric metabolite identifications can be ascertained with tandem MS/MS regarding the detected analytes compared with NMR. Furthermore, high-resolution MS can provide chemical formulations that can be used for putative matching of unknown metabolites using searchable databases such as the LIPID MAPS [25] and Human Metabolome [26] databases. To increase the selectivity of MS and reduce matrix effects, chromatography techniques such as gas chromatography (GC)-MS, capillary electrophoresis (CE)-MS, and liquid chromatography (LC)-MS are commonly placed in line with MS. GC-MS separates molecules in the gas phase with excellent reproducible retention. In addition, the consistent reproducible fragmentation patterns created by electron impact (EI) make molecular identification through database matching relatively simple [4]. However, GC-MS is disadvantaged in that only volatile and nonvolatile molecules that have been derivatized are acceptable for GC-MS analysis [3]. CE-MS is best used for the separation of charged polar metabolites [3] and it is suggested that lipids should be removed from the sample [27]. Alternatively, with the addition of a charged surfactant to CE, neutral molecules can be separated by micellar electrokinetic chromatography (MEKC) [24]. The reproducibility of CE is considered to be poor, unwanted electrochemical side reactions can take place, and it is not a robust technique [24]. LC-MS is widely used in metabolomics and often incorporates both reversed-phase (RP) and normal-phase

(NP) columns [3, 24]. The commonly used stationary phases of C₈ or C₁₈ in RP columns provide separation of lipids and other nonpolar metabolites in the extracted organic phase [24], while NP-LC can employ hydrophilic interaction chromatography (HILIC) to separate the more polar metabolites of the aqueous phase extract [24]. Both RPLC and HILIC can be used to expand the coverage of the metabolome, but two consecutive chromatographic separations increase both analysis time and cost [13, 28]. There are methods being developed to simultaneously separate polar and lipid metabolites using a single column, but thus far only lipids with polar head groups, such as glycerophospholipids, have been detected [13].

Historically, a separatory funnel has been used to separate polar and nonpolar molecules to determine a molecule's respective partition coefficient [29]. The partition coefficient, $\log K_{O/W}$, is a constant that describes a molecule's affinity for the organic or aqueous phase and is defined as the \log of the ratio of a molecule's concentration in the organic phase to the concentration in the aqueous phase using octanol and water at equilibrium [29]. When immiscible solvents other than octanol and water are implemented, the distribution ratio can be calculated to measure the partitioning of a solute. The distribution ratio, K_D, measured using the ratio of a molecule's concentration in the organic to aqueous phase of any immiscible solvent system regardless of equilibrium [29]. Once correlation coefficients based on a solute's retention factor are determined, the distribution ratios calculated by chromatography methods can then be used as predictors of partition coefficients for that solute [29, 30].

Analyses of the metabolome and/or lipidome incorporating biphasic mixtures are most prevalent in the analysis of biofluids and tissues resulting in data that is averaged over many cells. Techniques for the high-throughput analyses of single cells have been developed using printed microarrays [31], flow cytometry, microfluidics, and CE [2, 32, 33]. However, chromatographic separation by microfluidics and CE incurs lengthy run-times or purification steps. Flow cytometry is limited in the breadth of information acquired, and printed microarrays often result in the deposition of multiple cells [31] resulting in data averaged over multiple cells. NMR and Raman spectroscopy analysis of single cells are non-destructive techniques that provide real-time analysis of the dynamic metabolome. Raman is disadvantaged by the lack of molecular identifications it can provide [34], and NMR is disadvantaged by its sensitivity limitations of micro-molar analyte detection [4, 8], as previously stated.

Direct analyte-probed nanoextraction (DAPNe) is a method developed by our group for the extraction of trace materials in complex matrices using a nanomanipulation workstation coupled to nanoelectrospray ionization (NSI) for analysis by direct inject mass spectrometry (DIMS) [35–39]. The nanomanipulator is mounted on a microscope stage and is equipped with up to four nanopositioners driven by piezoelectric motors. Each of the positioners can be fitted with micro-electrodes, microgrippers, nanospray emitters, quartz rods, or glass capillaries. The positioners are controlled by a joystick in

the X-, Y-, and Z-axes with a spatial resolution of 100 nm and 5 nm in coarse and fine modes, respectively. The movement of the positioner allows for the precise extraction of the area of interest reducing matrix effects as well as the need for chromatographic separation or pretreatment of the sample [35, 38].

Recently, DAPNe of one cell has been used to identify lipid heterogeneity within breast tumor and adjacent healthy tissues [40, 41], mammalian cell culture [42], and plant tissues [43, 44]. DAPNe of one cell has been developed for the extraction of individual cells and/or organelles from individual cells and can be coupled to nanoelectrospray ionization (NSI)-MS [40–45], or matrix assisted laser desorption/ionization (MALDI)-Orbitrap-MS to image an extracted sample [45]. Here we describe for the first time the use of DAPNe using a glass micro-capillary tip as a separatory funnel coupled to MALDI-MS to image the distribution of solutes from a reaction mixture of phenethylamine analogues and a lipid standards mix, in a CHCl₃/H₂O solvent system to establish proof of principle. Ultimately, the method is demonstrated for the analysis of one cell as an untargeted lipid profiling method to analyze both polar and nonpolar lipids in a single extraction step while reducing ion suppression often found in direct lipid analysis of MALDI samples [46].

Materials and Methods

Phenethylamine Reaction Mixture

Following the procedure described by Clemons et al. [47], alkylated phenethylamine (PEA) analogues were synthesized using 1-iodomethane, 1-iodoethane, 1-iodopropane, 1-iodobutane, 1-iodopentane, 1-iodohexane, 1-iodoheptane, and 1-iodooctane; all from Sigma Aldrich (St. Louis, MO, USA). The synthesis resulted in a mixture of secondary and tertiary PEA analogues of varying alkyl moieties with 2–16 total carbons and primary PEA. The final reaction mixture is dissolved in 1:1 CHCl₃:MeOH (HPLC grade; Sigma-Aldrich).

Lipid Standards

Lipid standards including polar brain lipids, triheptadecanoate (17:0/17:0/17:0) (TG 51:0) (both from Avanti Polar Lipids, Alabaster, AL, USA), and triglycerol mix 2:0–10:0 (Sigma-Aldrich) were each dissolved in 1:1 CHCl₃:MeOH (HPLC grade (Sigma-Aldrich) and mixed to a final concentration of 2 μM for each standard.

Snu-5 Cells

Human gastric carcinoma cells, SNU-5 (ATCC CRL-5973, American Type Culture Collection (ATCC), Manassas, VA, USA), were cultured in suspension producing both individual cells and aggregates of multiple cells. The average diameter of an individual cell was found to be 20 μm through measurements using the Nikon Elements software package (Nikon, Melville, NY, USA). The cells were cultured at 37 °C under

5% CO₂ in Iscove's Modified Dulbecco's Medium supplemented with 20% fetal bovine serum (all from ATCC).

Extraction

Extractions, Figure 1a, were performed utilizing a modified nanomanipulator workstation (DCG Systems Inc., Fremont, CA, USA) mounted to an AZ100 microscope (Nikon). A single prober was fitted with a quartz capillary tip pulled using a P-2000 CO₂-laser micropipette puller (Sutter Instruments, Novato, CA, USA) to an internal diameter of 20 μm matching the average diameter of the Snu-5 cells to reduce the chance of damaging the cells and inducing unwanted responses from mechanical shearing during extraction.

For analysis of the lipid standards and drug mix (PEA analogues), 1 μL of a standard solution is backfilled into a capillary tip. A 1-μL droplet of 18Ω Milli-Q water (Millipore, Billerica, MA, USA) is deposited on a clean glass slide. Using the joystick controller, the capillary tip is then positioned directly above the water droplet and slowly lowered into the droplet. Using a pressure injector, the water is aspirated into the capillary tip and drawn through the standard solution, Figure 1a. The immiscible layers are allowed to separate before being spotted onto a stainless steel MALDI tissue slide, Figure 1b.

The procedure for the analysis of the suspension cells differs slightly from the standard solutions; 1 μL of the cell suspension was centrifuged to remove the growth media, and cells resuspended in ammonium carbonate buffer until extraction. First, the capillary tip is backfilled with 1 μL of CHCl₃, then positioned adjacent to a suspended Snu-5 cell within a droplet of cell suspension. Once in position, using a nitrogen gas pressure injector, negative pressure, −1.0 psi, is applied to draw the cell into the capillary tip, the cell is left to lyse within the solvent (~5 min), then 1 μL of water is aspirated into the capillary tip, and the phases are allowed to separate before being spotted.

Immediately after the spotted sample has evaporated, a second capillary tip filled with 2 μL of MALDI matrix, 20 mg/mL 2,5-dihydroxybenzoic acid (DHB) (DHB 98%, Sigma-Aldrich) solution in 3:2 acetonitrile/water (ACN/H₂O) (v/v), (HPLC grade, Sigma-Aldrich) is placed into the prober and positioned over the sample spot. Following the method described by Phelps et al. [45], DHB is then spotted onto the sample and dried with a stream of nitrogen before being loaded into the MALDI front end for analysis, Figure 1b.

MALDI-LTQ-Orbitrap Analysis

MALDI-MS experiments were conducted on a MALDI-LTQ-XL-Orbitrap (Thermo Scientific, San Jose, CA, USA) equipped with a 337 nm N2 laser (MNL 100; Lasertechnik, Berlin, Germany). Conditions were as follows: 15 μJ energy per laser shot, 1 laser shot per spectra, and laser raster motion was set at a 60 μm step size for lipid samples and 100 μm for drug sample. Data acquisition was collected in positive ion mode using a mass range of *m/z* 100–1100 (lipids), and *m/z* 50–600

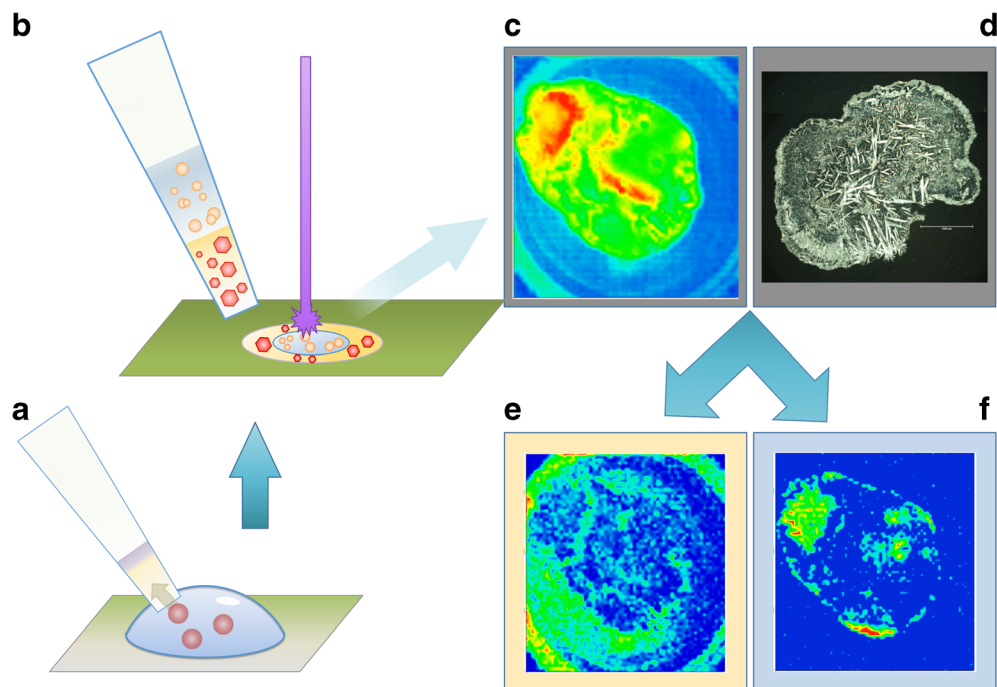


Figure 1. Illustration representing the DAPNe-micro-capillary separation-MALDI-MS imaging method. Use of DAPNe for the extraction of one cell using a micro-capillary backfilled with 1 μL of organic solvent (**a**), followed by aspiration of 1 μL water for metabolite partitioning in an immiscible solvent system. Upon phase separation (**b**), the phases are spotted onto a MALDI slide, evaporated, and spotted with matrix for MALDI-MS imaging. The resulting total ion count (TIC) represents the overall shape of the sample spot and peak selection displays the distribution of that peak to the organic phase (**d**) or aqueous phase (**e**)

(drug), with a mass resolution of 60,000 (at m/z 400). Data processing was performed using Xcalibur ver. 2.3 (Thermo Scientific). Image processing for the deposited spots was performed with ImageQuest ver. 1.1, (Thermo Scientific) the mass range plotted, and linear smoothing applied, Figure 1c–e. Mass spectra were plotted using PSI-Plot software (Poly Software International, Pearl River, NY, USA).

Distribution Ratio (K_D)

To evaluate the partitioning of various solutes, the distribution ratio was calculated as the ratio of the total ion count of an analyte in the organic phase (chloroform) to the total ion count of the same analyte in the aqueous phase (water). This was performed using the polygonal selection tool of the MSI software suite [48] to highlight each phase of the MALDI-MS images separately. The mass spectral data for each scan within the selected area was exported and the absolute intensity of a specific peak was summed for each phase. The total intensity for both the organic and aqueous regions of the image, Table 1, were then used to calculate the distribution ratio, K_D , and the log of the ratio taken, $\log K_D$ using Equations 1 and 2, respectively.

$$K_D = \frac{[\text{CHCl}_3]}{[\text{H}_2\text{O}]} \quad (1)$$

$$\log K_D = \log 10 \left(\frac{[\text{CHCl}_3]}{[\text{H}_2\text{O}]} \right) \quad (2)$$

The data in Table 1b and c, columns $[\text{CHCl}_3]$, $[\text{H}_2\text{O}]$, K_D , and $\log K_D$, were calculated based on all possible adducts associated with each lipid species ($[\text{M} + \text{H}]^+$, $[\text{M} + \text{Na}]^+$, and/or $[\text{M} + \text{K}]^+$). The ion column indicates which adduct was used to create the MALDI images found in Figures 3 and 4.

Results and Discussion

During the drying process of the MALDI spots, it was determined that the aqueous phase remained in the center of the spot as the organic phase spread outward from the origin of the spotting position. While the center of the MALDI images is the aqueous phase, some aggregation of hydrophobic molecules can be found within this phase because of the density and evaporation rate of the chloroform. During the spotting and phase separations, the chloroform was expelled from the capillary tip first, followed by the water. The surface tension of the chloroform is such that it does not form a droplet but rather spreads out radially, in effect increasing the surface to air ratio causing the chloroform evaporation to speed up. This resulted in the deposition of some chloroform soluble analytes beneath the aqueous phase, thus providing the illusion that some organic phase analytes dispersed into the aqueous phase. This was not corrected for when calculating the distribution ratios.

Table 1. Tabulated Information for Calculation of K_D and Peak Identification in Spectra

(a) Phenethylamine (PEA) analogues							
Figure 1	Peak ($m/z \pm 0.003$)	ID/carbon no.	Ion	[CHCl ₃]	[H ₂ O]	K_D	log K_D
a	122.097	PEA	[M+H] ⁺	4.67E+06	2.38E+07	0.196	-0.708
b	150.128	2C	[M+H] ⁺	1.37E+06	1.09E+07	0.125	-0.902
c	164.144	3C	[M+H] ⁺	5.63E+07	3.72E+08	0.151	-0.820
d	178.160	4C	[M+H] ⁺	6.02E+07	3.23E+08	0.186	-0.730
e	192.175	5C	[M+H] ⁺	5.91E+07	2.24E+08	0.264	-0.579
f	206.191	6C	[M+H] ⁺	1.81E+08	4.71E+08	0.384	-0.415
g	220.207	7C	[M+H] ⁺	3.17E+08	6.02E+08	0.527	-0.278
h	234.222	8C	[M+H] ⁺	5.87E+08	7.51E+08	0.781	-0.107
i	248.238	9C	[M+H] ⁺	1.02E+09	8.40E+08	1.214	0.084
j	262.254	10C	[M+H] ⁺	2.32E+09	1.43E+09	1.618	0.209
k	276.269	11C	[M+H] ⁺	2.64E+09	1.15E+09	2.294	0.361
l	290.285	12C	[M+H] ⁺	2.72E+09	9.57E+08	2.847	0.454
m	304.300	13C	[M+H] ⁺	2.31E+09	6.34E+08	3.637	0.561
n	318.316	14C	[M+H] ⁺	1.36E+09	3.14E+08	4.333	0.637
o	346.347	16C	[M+H] ⁺	3.29E+08	4.94E+07	6.663	0.824
b. Lipid standard mixture							
Figure 3	Peak ($m/z \pm 0.003$)	Known ID	Ion	[CHCl ₃]	[H ₂ O]	K_D	log K_D
a	325.162	TG (12:0)	[M+NA] ⁺	3.06E+05	8.43E+05	0.363	-0.440
b	409.256	TG (18:0)	[M+NA] ⁺	6.76E+05	1.30E+06	0.522	-0.283
c	493.350	TG (24:0)	[M+NA] ⁺	7.07E+08	2.11E+08	3.347	0.525
d	577.444	TG (30:)	[M+NA] ⁺	5.15E+08	1.14E+08	4.501	0.653
e	871.773	TG (51:0)	[M+NA] ⁺	8.10E+07	3.55E+07	2.281	0.358
f	377.168	LPA (12:0)	[M+NA] ⁺	1.48E+07	4.19E+07	0.354	-0.451
g	496.340	LPC(16:0)	[M+H] ⁺	2.35E+06	4.82E+04	48.745	1.688
h	637.332	LPI (19:0)	[M+NA] ⁺	7.81E+05	2.35E+06	0.332	-0.478
i	723.495	PA(36:2)	[M+Na] ⁺	5.30E+05	2.36E+04	22.425	1.350
j	782.570	PC(34:1)	[M+Na] ⁺	2.97E+05	1.31E+04	22.666	1.355
(c) Snu-5 one-cell extraction							
Figure 4	Peak ($m/z \pm 0.003$)	Known ID	Ion	[CHCl ₃]	[H ₂ O]	K_D	log K_D
-	257.248	FA(16:0)	[M+H]	16594783.16	7.97E+06	2.082	0.319
a	281.245	FA(18:2)	[M+H]	5.61E+10	5.44E+10	1.030	0.013
-	285.2788	FA(18:0)	[M+H]	2.48E+06	1.00E+06	2.475	0.394
-	588.536	Cer(d36:1)	[M+Na]	1.43E+06	4.89E+05	2.923	0.466
b	618.580	Cer(d38:0)	[M+Na]	1.58E+09	2.24E+09	0.706	-0.151
c	734.570	PC(32:0)	[M+H]	9.17E+06	3.31E+07	0.277	-0.557
d	758.570	PC(34:2)	[M+H]	1.57E+06	5.51E+05	2.850	0.455
e	782.568	PC(34:1)	[M+Na]	1.91E+06	1.50E+07	0.127	-0.896
f	784.583	PC(34:0)	[M+Na]	4.40E+06	2.11E+07	0.209	-0.679
g	810.599	PC(36:1)	[M+Na]	2.10E+06	6.93E+06	0.302	-0.519
h	728.463	PE(32:1)	[M+K]	1.01E+06	7.20E+05	1.409	0.149
i	692.523	PE(32:0)	[M+H]	1.54E+06	8.87E+05	1.732	0.239
j	742.536	PE(34:0)	[M+Na]	2.82E+06	1.00E+06	2.821	0.450
k	770.568	PE(36:0)	[M+Na]	1.81E+06	1.82E+06	0.997	-0.001
l	661.533	CE(16:1)	[M+K]	5.04E+08	3.15E+08	1.598	0.204
m	689.564	CE(18:1)	[M+K]	5.05E+08	3.69E+08	1.370	0.137
n	967.868	TG(58:1)	[M+Na]	1.46E+08	8.25E+07	1.767	0.247
o	1009.856	TG(60:2)	[M+K]	1.48E+08	8.80E+07	1.687	0.227

TG = triglyceride; LPA = lysophosphatidic acid; PA = phosphatidic acid; PC = phosphatidylcholine; PE = phosphatidylethanolamine; FA = fatty acid; Cer = ceramide; CE = cholesterol ester

Drug Spots

The dispersion of the PEA analogues between the two phases correlates with the total number of carbons in the acyl moieties of the alkylated PEA such that as the carbon number increases, the dispersion from the aqueous phase to the organic phase also increases, as can be seen in Figure 2. The images of Figure 2b–n differ by the addition of a single carbon to the acyl moieties of the PEA analogue from two to 14 carbons and a total of 16 carbons in Figure 2o, as denoted in Table 1a. It is important to note that secondary PEA analogues exist within the analytes detected in Figure 2b–h. These secondary species are expected to partition between the

aqueous and organic phases despite an increasing alkyl chain as observed in Figure 2g and h. Figure 2a, m/z 122.0970, shows the predominant partition into the aqueous phase of phenethylamine, a primary amine. The secondary and tertiary PEA analogues with two total substituted carbons also partition strongly within the aqueous phase, as seen in Figure 2b, m/z 150.1283. With a total substituted carbon count of seven, Figure 2g, the analytes begin to partition into the organic phase. Figure 2j illustrates a relatively even partitioning of tertiary PEA analogues with 10 total carbons in which an ethyl is the shortest alkyl chain. This trend of an increased partition into the organic phase continues as the total number of carbons added to the alkylated PEA analogues

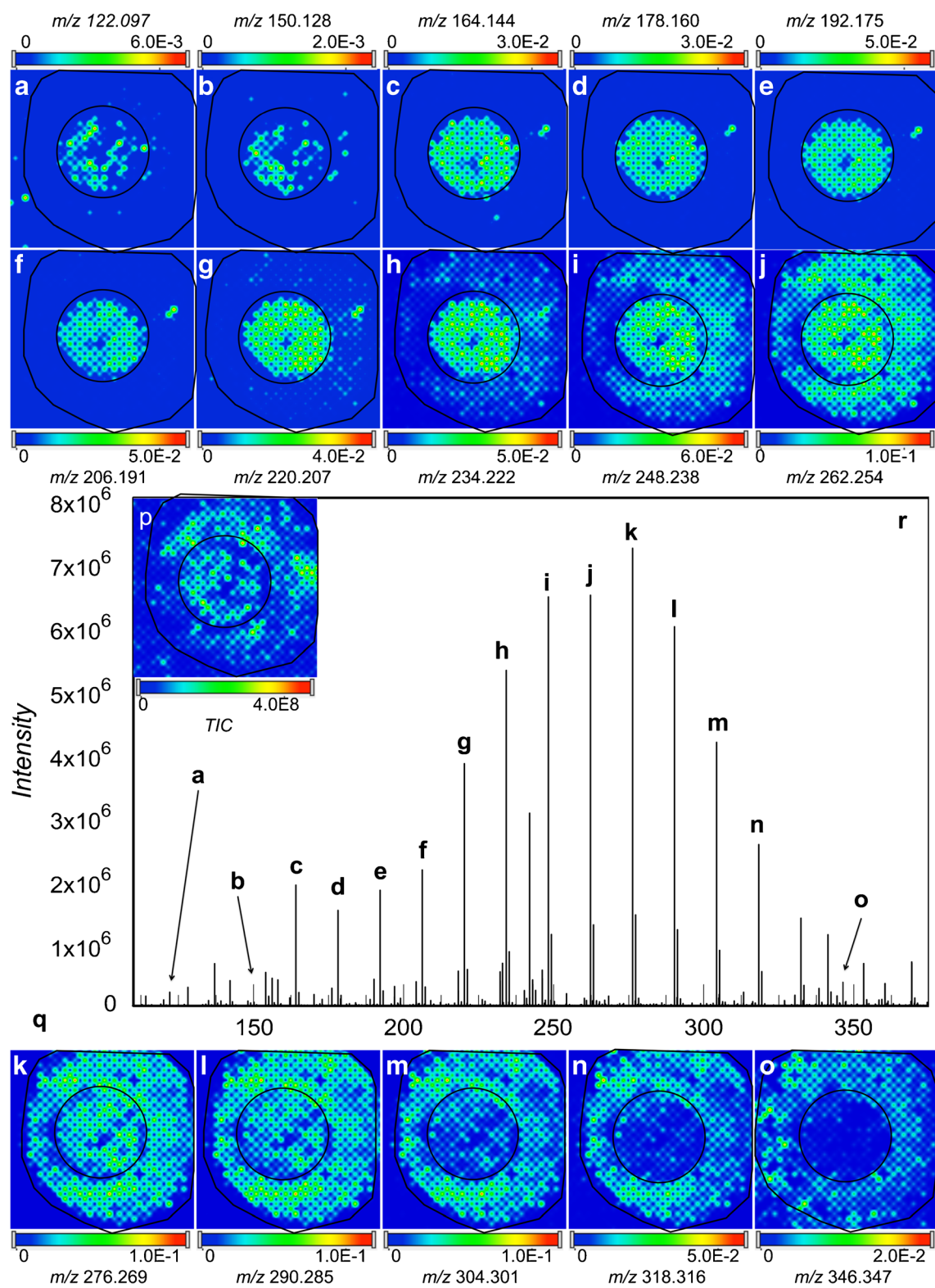


Figure 2. (a)-(j) (a)-(o) MALDI images of selected peaks of phenethylamine (PEA) analogues for the visualization of their respective phase partitioning. (p) The total ion count of the PEA reaction mixture sample spot. Identified peaks of most abundant PEA analogues within an averaged spectrum (q)

increases, Figure 2k-o. The partitioning trend is also expressed by the $\log K_D$ values found in Table 1a, which range from -0.708 to 0.824 for m/z 122.0970

and m/z 346.3474, respectively. The drug spot analysis provides evidence for the ability of this method to provide a visual partitioning of molecules with minimal

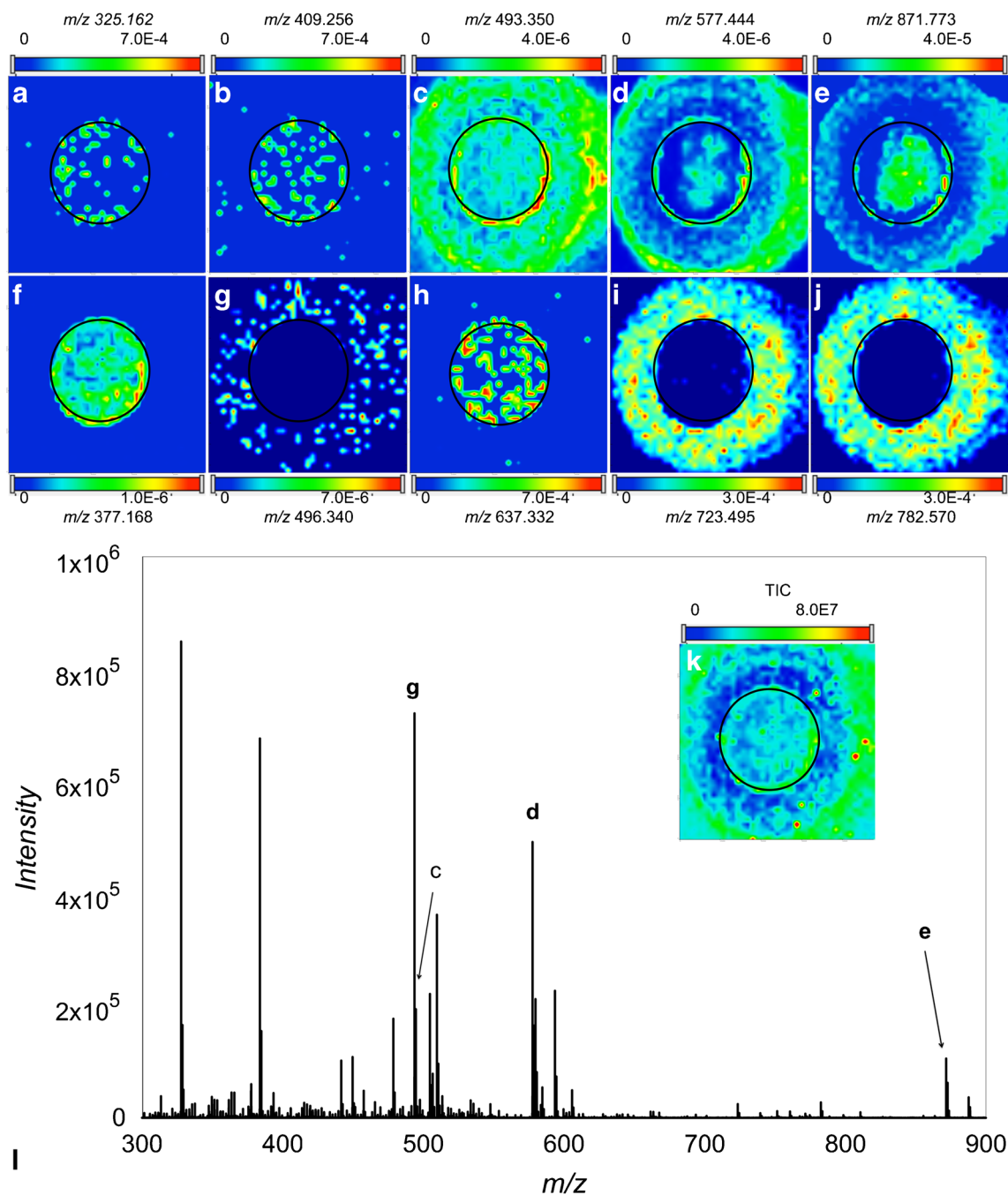


Figure 3. (a)–(j) Selected peaks of known lipid species in a lipid standard mixture for visualization of their respective phase partitioning. (k) The total ion count of the lipid standard mixture sample spot. (l) Identified peaks of most abundant expected lipid

increases in hydrophobic character based on their increased distribution into the organic phase of the solvent system.

Lipid Spot

The dispersion of the triglyceride (TG) standards in the aqueous and/or organic regions within the spots is relative to the fatty acyl chain length of the TG and can be seen in the images of Figure 3 and supported by the $\log K_D$ values in Table 1b.

The TG (12:0) standard (Figure 3a) was localized in the aqueous phase with a $\log K_D$ of -1.11, and the TG (51:0) standard (Figure 3e) was localized more in the organic phase, with a $\log K_D$ of 0.33. The polar brain lipid standards were found in both the aqueous and organic phases. Lysophosphatidic acid (LPA) (Figure 3f), with its polar head group and relatively short 12-carbon acyl chain, migrated more to the aqueous phase and has a $\log K_D$ value of -0.91. Lysophosphatidylcholine (16:0) [LPC(16:0)] (Figure 3g) partitions more in the organic phase with a $\log K_D$ of 1.688, and is a result of its longer 16-carbon

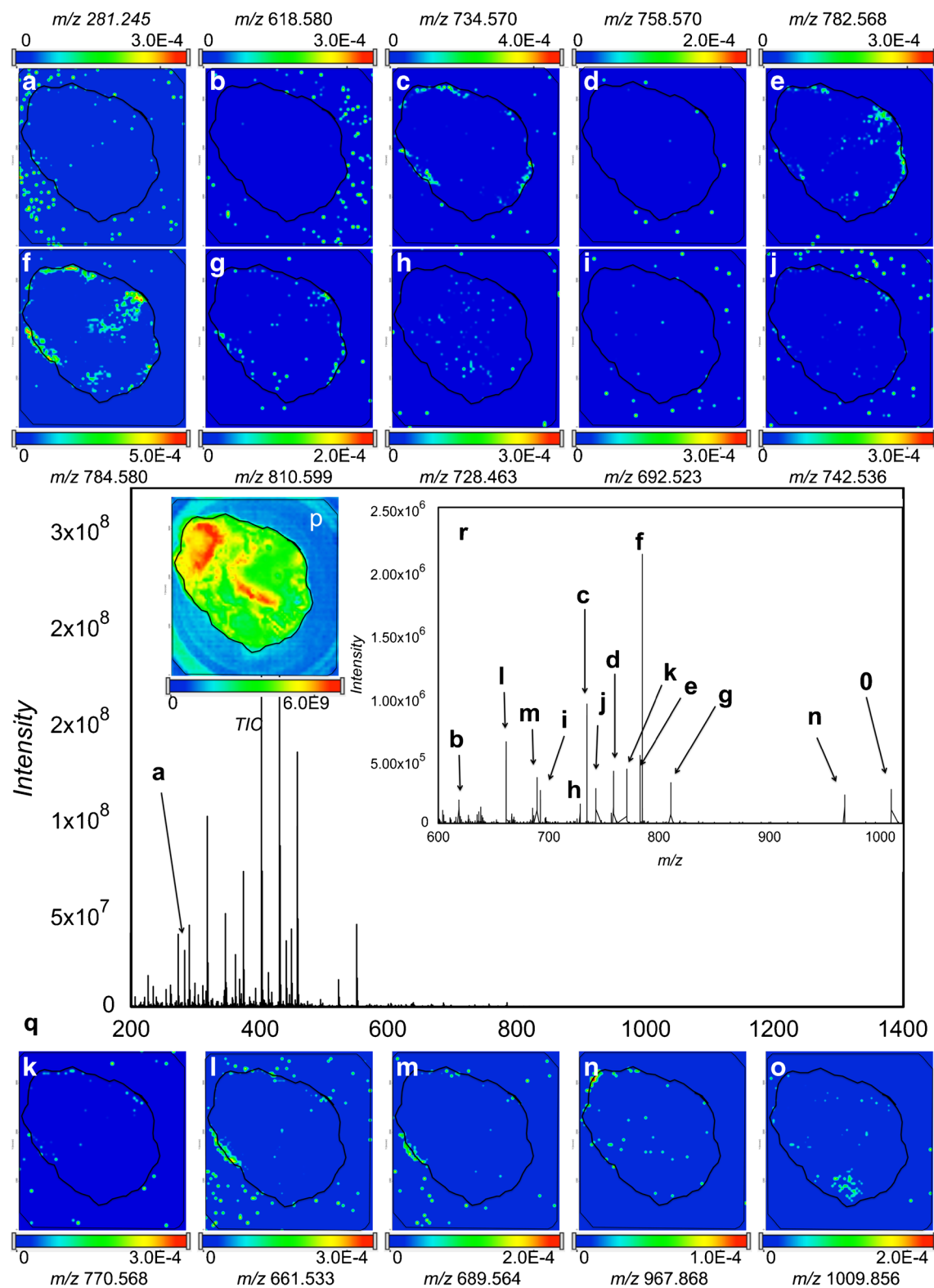


Figure 4. (a)–(o) MALDI images of selected peaks of putatively identified lipid species from the one-cell extraction of a Snu-5 cell for visualization of their respective phase partitioning. (p) The total ion count of the one-cell extraction sample spot. (q) Identified peaks of selected putatively identified lipids within an averaged spectrum, with inset (r) of peaks greater than m/z 600

acyl chain and less polar head group, compared with LPA. The distribution of the lipid standards is correlated to the acyl chain

length of the fatty acyl constituents as well as the nature of the head group for the specific lipids described here.

Snu-5 Whole Cell

The MALDI-MS analysis of lipids extracted from an intact individual Snu-5 gastric cancer cell resulted in the detection of multiple lipid classes, including glycerophospholipids, ceramides, cholesterol esters, triglycerides, and fatty acids in the positive mode using the MALDI matrix 2,5-DHB. Select peaks of interest were putatively identified through a Lipid MAPS database search of protonated, sodiated, or potassium neutral and polar lipid species with a tolerance of $m/z \pm 0.005$. Distribution ratios for 18 peaks of interest were calculated, Table 1c, and visual partitioning of 15 putative matches are represented as MALDI images, Figure 4a–o. The center of the Snu-5 MALDI spot was determined to be the aqueous phase. An irregular oval-shaped black line was drawn around the center region of each MALDI image in Figure 4 to show where the inner aqueous phase meets the outer organic phase.

Of the 18 peaks reported here, five were found to be phosphatidylcholine, making it the most represented lipid class within the single-cell extract. The partitioning of the PC species resulted in an aggregation near where the aqueous and organic phases meet. The calculated $\log K_D$ values of the PC species ranged from –0.161 to 0.318, Table 1c. Four masses of interest were putatively identified as phosphatidylethanolamine, making it the second most represented class of lipids. The PE species appear to partition into both phases and appear to not aggregate within a specific area of the sample spot. The identification of nine glycerophospholipids is not surprising as they are readily associated with cellular membranes and should be expected to account for a larger portion of the cellular lipid population.

Contrary to the PE species, two cholesterol ester peaks, m/z 661.533 and 686.564, are shown to aggregate heavily to a single region, forming a relatively concentrated pocket along the organic side of the biphasic line within the MALDI spot, Figure 4l and m. It is of interest to note that the hydrophilic triglyceride species, m/z 967.868 and 1009.856, partitioned within the aqueous region of the spot, Figure 4n and o. The partitioning of these neutral lipids can best be explained as a result of the drying process described at the beginning of the “Results and Discussion” section.

The identification of Cer (d38:0), Figure 4b, is of interest as it has been reported to be formed in response to apoptosis within a cell [26], and suggests the addition of a quenching step prior to extraction is required. Quenching is performed through pretreatments of a sample with an organic solvent. Dietmar et al. performed a comparison study of 12 metabolite extraction procedures coupled with several quenching methods and determined that a pretreatment with cold 0.9% NaCl is the only acceptable quenching method for mammalian cells as all other methods tested resulted in cell membrane damage that lead to metabolite leakage [21].

Although the lipid species of the Snu-5 one-cell analysis were putatively identified through an exact mass search of the

LIPID MAPS database [25] with a mass tolerance of 0.005 Da; tandem MS should be performed to elucidate chemical structures for confirmation of identification. Tandem MS using electrospray ionization (ESI) or NSI can be difficult to perform on single-cell samples due to small sample volumes ($\leq 10 \mu\text{L}$) and limited analysis times (~2 min). The use of DAPNe-micro-capillary separatory chemistry-MALDI-MS for the spotting of extracts for MALDI imaging provides an increase in the amount of time that can be spent with a sample compared with other methods such as NSI-MS; in fact, Phelps et al. reported a 15-fold increase in analysis time when coupling DAPNe to MALDI-MS [45]. Furthermore, Phelps et al. demonstrated the ability to reanalyze the MALDI sample spot using tandem MS to verify the identification of analytes of interest [45]. This increase in time allows for more thoughtful and thorough processing of the data and offers the benefit of multiple MALDI analyses. Unfortunately, due to the length of time between putative database identification and original analysis, the MALDI spots were not reanalyzed for structural confirmation of putative identifications.

During immiscible solvent extraction, semipolar metabolites can disperse into both the organic and aqueous phases [3]. If a procedure requires the collection and purification of each phase separately for separation by RP-LC and NP-LC, one or both of the methods may not be suitable for these semipolar metabolites, resulting in their elution in the dead volume preventing their detection in the sample [13]. DAPNe-micro-capillary separatory chemistry-MALDI-MS removes the need for phase collection and purification steps as well as chromatographic separations, meaning the entire organic and aqueous phases are retained and deposited on the MALDI slide for simultaneous analysis. Furthermore, separation prior to MALDI-MS analysis has been shown to reduce the ion suppression effect of the phosphatidylcholine species on other lipid classes [46]. In a review of MALDI-MS characterization of lipids, it was reported that the presence of PC can severely suppress neutral lipids such as triglycerides [46]. However, with the use of solid phase extraction, this suppression is significantly reduced and TG species ion intensities are more representative of their actual abundance within a sample. Using DAPNe-micro-capillary separatory chemistry-MALDI-MS for lipid analysis PC, PE, TG, and CE lipid species are all identified with ion intensities on the same order of magnitude when normalized to the total ion count. Therefore, the use of immiscible solvents for the partitioning of polar and nonpolar lipids during one-cell analysis provides a method for separations when chromatographic methods are infeasible.

It is of interest to note that the use of micro-capillary phase separation using immiscible solvents was previously attempted in our lab using NSI. The technique described in previous papers, DAPNe-NSI-MS [40, 41, 45], was not compatible with immiscible phase separation within a micro-capillary emitter as the change in phases caused an interruption in sample flow and the aqueous phase remained in the capillary emitter during analysis with NSI.

Conclusion

The coupling of DAPNe to micro-capillary separatory chemistry with MALDI-MS imaging demonstrates a technique capable of increasing the range of polar and nonpolar molecules that can be analyzed simultaneously using a single step extraction method of one-cell without pretreatment or chromatography separations. The spotting of one-cell extracts on a MALDI slide for imaging not only allows reanalysis of the sample but also provides visual confirmation that partitioning of hydrophilic and lipophilic molecules occurs within the micro-capillary during extraction. However, to reduce the unexpected partitioning of hydrophilic molecules within the aqueous phase, the MALDI spotting method needs optimization. Furthermore, due to limitations of our instrument, fast polarity switching was not available and therefore analysis was not performed in the negative mode. However, to fully examine the method described here, the analysis of both positive and negative ions should be considered, along with performance evaluations of other multiphasic solvent systems for enriched lipid extraction and enhanced biomarker discovery.

Acknowledgements

The authors acknowledge support for this work by the CPRIT High-Impact Research Award (RFA R-13-HIHR-1). The authors thank Dr. Kent Chapman and Mr. Drew Sturtevant for direction in lipid metabolism.

References

- Rubakhin, S.S., Romanova, E.V., Nemes, P., Sweedler, J.V.: Profiling metabolites and peptides in single cells. *Nat. Methods* **8**, S20–S29 (2011)
- Zenobi, R.: Single-cell metabolomics: analytical and biological perspectives. *Science* **342**, 1243259 (2013)
- Cajka, T., Fiehn, O.: Toward merging untargeted and targeted methods in mass spectrometry-based metabolomics and lipidomics. *Anal. Chem.* **88**, 524–545 (2016)
- Peng, B., Li, H., Peng, X.-X.: Functional metabolomics: from biomarker discovery to metabolome reprogramming. *Protein Cell* **6**, 628–637 (2015)
- Meikle, P., Barlow, C., Weir, J.: Lipidomics and lipid biomarker discovery. *Austral. Biochem.* **40**, 12–16 (2009)
- Zhou, X., Mao, J., Ai, J., Deng, Y., Roth, M.R., Pound, C.: Identification of plasma lipid biomarkers for prostate cancer by lipidomics and bioinformatics. *PLoS One* **7**, e48889 (2012)
- Shah, S.H., Kraus, W.E., Newgard, C.B.: Metabolomic profiling for the identification of novel biomarkers and mechanisms related to common cardiovascular diseases. *Circulation* **126**, 1110–1120 (2012)
- Armitage, E.G., Barbas, C.: Metabolomics in cancer biomarker discovery: current trends and future perspectives. *J. Pharm. Biomed. Anal.* **87**, 1–11 (2014)
- Folch, J., Lees, M., Stanley, G.H.S.: A simple method for the isolation and purification of total lipids from animal tissues. *J. Biol. Chem.* **226**, 497–509 (1957)
- Bligh, E.G., Dyer, W.J.: A rapid method of total lipid extraction and purification. *Can. J. Biochem. Physiol.* **37**, 911–917 (1959)
- Tyagi, R.K., Azrad, A., Degani, H., Saloman, Y.: Simultaneous extraction of cellular lipids and water-soluble metabolites: evaluation by NMR spectroscopy. *Magn. Reson. Med.* **35**, 194–200 (1996)
- Creek, D.J., Jankevics, A., Breitling, R., Watson, D.G., Barrett, M.P., Burgess, K.E.V.: Toward global metabolomics analysis with hydrophilic interaction liquid chromatography-mass spectrometry: improved metabolite identification by retention time prediction. *Anal. Chem.* **83**, 8703–8710 (2011)
- Fei, F., Bowdish, D.M.E., McCarry, B.E.: Comprehensive and simultaneous coverage of lipid and polar metabolites for endogenous cellular metabolomics using HILIC-TOF-MS. *Anal. Bioanal. Chem.* **406**, 3723–3733 (2014)
- Byeon, S.K., Lee, J.Y., Lee, J.-S., Moon, M.H.: Lipidomic profiling of plasma and urine from patients with Gaucher disease during enzyme replacement therapy by nanoflow liquid chromatography-tandem mass spectrometry. *J. Chromatogr. A* **1381**, 132–139 (2015)
- Patterson, R.E., Ducrocq, A.J., McDougall, D.J., Garrett, T.J.: Comparison of blood plasma sample preparation methods for combined LC-MS lipidomics and metabolomics. *J. Chromatogr. B* **1002**, 260–266 (2015)
- Yang, Y., Cruickshank, C., Armstrong, M., Mahaffey, S., Reisdorff, R., Reisdorff, N.: New sample preparation approach for mass spectrometry-based profiling of plasma results in improved coverage of metabolome. *J. Chromatogr. A* **1300**, 217–226 (2013)
- Whiley, L., Godzien, J., Ruperez, F.J., Legido-Quigley, C., Barbas, C.: In-vial dual extraction for direct LC-MS analysis of plasma for comprehensive and highly reproducible metabolic fingerprinting. *Anal. Chem.* **84**, 5992–5999 (2012)
- Chen, S., Hoene, M., Li, J., Li, Y., Zhao, X., Haring, H.-U.: Simultaneous extraction of metabolome and lipidome with methyl tert-butyl ether from single small tissue sample for ultra-high performance liquid chromatography/mass spectrometry. *J. Chromatogr. A* **1298**, 9–16 (2013)
- Godzien, J., Cibrowski, M., Whiley, L., Legido-Quigley, C., Ruperez, F.J., Barbas, C.: In-vial dual extraction chromatography coupled to mass spectrometry applied to streptozotocin-treated diabetic rats. Tips and pitfalls of the method. *J. Chromatogr. A* **1304**, 52–60 (2013)
- Sen, A., Wang, Y., Chiu, K., Whiley, L., Cowan, D., Chang, R.C.-C.: Metabolic phenotype of the healthy rodent model using in-vial dual extraction of dried serum, urine, and cerebrospinal fluid spots. *Anal. Chem.* **85**, 7257–7263 (2013)
- Dietmar, S., Timmins, N.E., Gray, P.P., Nielsen, L.K., Kromer, J.O.: Towards quantitative metabolomics of mammalian cells: development of a metabolite extraction protocol. *Anal. Biochem.* **404**, 155–164 (2010)
- Ivanisevic, J., Zhu, Z.-J., Plate, L., Tautenhahn, R., Chen, S., O'Brien, P.J.: Toward 'omic scale metabolite profiling: a dual separation-mass spectrometry approach for coverage of lipid and central carbon metabolism. *Anal. Chem.* **85**, 6876–6884 (2013)
- Kirkwood, J.S., Maier, C., Stevens, J.F.: Simultaneous, untargeted metabolic profiling of polar and nonpolar metabolites by LC-Q-TOF mass spectrometry. *Curr. Protoc. Toxicol.* **56**, 4.39.31–4.39.12 (2013)
- Lei, Z., Huhman, D.V., Sumner, L.W.: Mass spectrometry strategies in metabolomics. *J. Biol. Chem.* **286**, 25435–25442 (2011)
- Sud, M., Fahy, E., Cotter, D., Brown, A., Dennis, E.A., Glass, C.K.: LMSD: LIPID MAPS structure database. *Nucleic Acids Res.* **35**, D527–D532 (2007)
- Wishart, D.S., Jewison, T., Guo, A.C., Wilson, M., Knox, C., Liu, Y.: HMDB 3.0—The human metabolome database in 2013. *Nucleic Acids Res.* **41**, D801–D807 (2013)
- Hirayama, A., Wakayama, M., Soga, T.: Metabolome analysis based on capillary electrophoresis-mass spectrometry. *Trends Anal. Chem.* **61**, 215–222 (2014)
- Wang, Y., Lehmann, R., Lu, X., Zhao, X., Xu, G.: Novel, fully automatic hydrophilic interaction/reversed-phase column-switching high-performance liquid chromatographic system for the complementary analysis of polar and apolar compounds in complex samples. *J. Chromatogr. A* **1204**, 28–34 (2008)
- Berthod, A., Carda-Broch, S.: Determination of liquid-liquid partition coefficients by separation methods. *J. Chromatogr. A* **1037**, 3–14 (2004)
- Poole, S.K., Poole, C.F.: Separation methods for estimating octanol-water partition coefficients. *J. Chromatogr. B* **797**, 3–19 (2003)
- Ellis, S.R., Ferris, C.J., Gilmore, K.J., Mitchell, T.W., Blanksby, S.J., Panhuis, M.I.H.: Direct lipid profiling of single cells from inkjet printed microarrays. *Anal. Chem.* **84**, 9679–9683 (2012)
- Trouillon, R., Passarelli, M.K., Wang, J., Kurczy, M.E., Ewing, A.G.: Chemical analysis of single cells. *Anal. Chem.* **85**, 522–542 (2013)
- Rubakhin, S.S., Lanni, E.J., Sweedler, J.V.: Progress toward single cell metabolomics. *Curr. Opin. Biotechnol.* **24**, 95–104 (2013)
- Wu, H., Volponi, J.V., Oliver, A.E., Parikh, A.N., Simmons, B.A., Singh, S.: In vivo lipidomics using single-cell Raman spectroscopy. *Proc. Natl. Acad. Sci. U. S. A.* **108**, 3809–3814 (2011)

35. Ledbetter, N.L., Walton, B.L., Davila, P., Hoffmann, W.D., Ernest, R.N., Verbeck, G.F.: Nanomanipulation-coupled nanospray mass spectrometry applied to the extraction and analysis of trace analytes found on fibers. *J. Forensic Sci.* **55**, 1218–1221 (2010)
36. Wallace, N., Hueske, E., Verbeck, G.F.: Ultra-trace analysis of illicit drugs from transfer of an electrostatic lift. *Sci. Justice* **51**, 196–203 (2011)
37. Clemons, K., Wiley, R., Waverka, K., Fox, J., Dziekonski, E., Verbeck, G.F.: Direct analyte-probed nanoextraction coupled to nanospray ionization-mass spectrometry of drug residues from latent fingerprints. *J. Forensic Sci.* **58**, 875–880 (2013)
38. Clemons, K., Nnaji, C., Verbeck, G.F.: Overcoming selectivity and sensitivity issues of direct inject electrospray mass spectrometry via DAPNe-NSI-MS. *J. Am. Soc. Mass Spectrom.* **25**, 705–711 (2014)
39. Clemons, K., Dake, J., Sisco, E., Verbeck, G.F.: Trace analysis of energetic materials via direct analyte-probed nanoextraction coupled to direct analysis in real time mass spectrometry. *Forensic Sci. Int.* **231**, 98–101 (2013)
40. Phelps, M., Hamilton, J., Verbeck, G.F.: Nanomanipulation-coupled nanospray mass spectrometry as an approach for single cell analysis. *Rev. Sci. Instrum.* **85**, 124101 (2014)
41. Hamilton, J.S., Verbeck, G.F.: One-cell analysis as a technique for true single-cell analysis of organelles in breast tumor and adjacent normal tissue to profile fatty acid composition of triglyceride species. *J. Anal. Oncol.* **5**, 47–54 (2016)
42. Phelps, M.S., Verbeck, G.F.: A lipidomics demonstration of the importance of single cell analysis. *Anal. Methods* **7**, 3668–3670 (2015)
43. Horn, P.J., Ledbetter, N.R., James, C.N., Hoffmann, W.D., Case, C.R., Verbeck, G.F.: Visualization of lipid droplet composition by direct organelle mass spectrometry. *J. Biol. Chem.* **286**, 3298–3306 (2011)
44. Horn, P.J., Joshi, U., Behrendt, A.K., Chapman, K.D., Verbeck, G.F.: On-stage liquid-phase lipid microextraction coupled to nanospray mass spectrometry for detailed, nano-scale lipid analysis. *Rapid Commun. Mass Spectrom.* **26**, 957–962 (2012)
45. Phelps, M.S., Sturtevant, D., Chapman, K.D., Verbeck, G.F.: Nanomanipulation-coupled matrix-assisted laser desorption/ionization-direct organelle mass spectrometry: a technique for the detailed analysis of single organelles. *J. Am. Soc. Mass Spectrom.* **27**, 187–193 (2016)
46. Lay, J.O., Gidden, J., Liyanage, R., Emerson, B., Durham, B.: Rapid characterization of lipids by MALDI MS. Part 2: artifacts, ion suppression, and TLC MALDI imaging. *Lipid Technol.* **24**, 36–40 (2012)
47. Clemons, K., Kretsch, A., Verbeck, G.F.: Parallel artificial membrane permeability assay for blood-brain permeability determination of illicit drugs and synthetic analogues. *Sci. Justice* **54**, 351–355 (2014)
48. Robichaud, G., Garrard, K.P., Barry, J.A., Muddiman, D.C.: MSiReader: an open-source interface to view and analyze high resolving power MS imaging files on Matlab platform. *J. Am. Soc. Mass Spectrom.* **24**, 718–721 (2013)